

Intense star cluster formation: stellar masses, the mass function, and the fundamental mass scale

CHRISTOPHER D. MATZNER¹

¹*David A. Dunlap Dept. of Astronomy and Astrophysics, University of Toronto, 50 St. George Street, Toronto, Ontario, M5S 3H4, Canada*

ABSTRACT

Within the birth environment of a massive globular cluster, the combination of a luminous young stellar population and a high column density induces a state in which the thermal optical depth and radiation pressure are both appreciable. In this state, the sonic mass scale, which influences the peak of the stellar mass function, is tied to a fundamental scale composed of the Planck mass and the mass per particle. Thermal feedback also affects the opacity-limited minimum mass and affects how protostellar outflows and binary fragmentation modify stellar masses. Considering the regions that collapse to form massive stars, we argue that thermal stabilization is likely to flatten the high-mass slope of the initial mass function. Among regions that are optically thick to thermal radiation, we expect the stellar population to become increasingly top-heavy at higher column densities, although this effect can be offset by lowering the metallicity. A toy model is presented that demonstrates these effects, and in which radiation pressure leads to gas dispersal before all of the mass is converted into stars.

1. INTRODUCTION

We wish to examine how environment affects the stellar initial mass function (IMF) during intense bursts of star cluster formation like those that give rise to massive globular clusters. Along the way, we will explore link between the peak of the IMF and the fundamental mass scales of stellar evolution.

The IMF $\psi(m_*) \propto d\dot{N}_*/dm_*$ is remarkably consistent in many well studied environments (Chabrier 2003), featuring a roughly log-normal distribution at low masses with a peak in $d\dot{N}_*/d\log m_* \propto m_*\psi(m_*)$ around $0.2M_\odot$ and a power law decline to high masses, $\psi \propto m_*^{-\alpha_{\text{high}}}$ (with $\alpha_{\text{high}} \simeq 2.35$ for $m_* > M_\odot$) which meets a cutoff somewhat above 10^2M_\odot . However, in some cases massive stars appear to be over-represented in the birth distribution. Examples from the inner Milky Way include the Arches (Hosek et al. 2019) and the young stars at the Galactic Center (Nayakshin & Sunyaev 2005; Lu et al. 2013).

There are now many extragalactic examples as well. An overabundance of massive stars is one plausible explanation for the unexpectedly numerous high-redshift ultraviolet sources discovered by JWST (Fujimoto et al. 2023). Very massive stars ($m_* > 100M_\odot$) are copious wind sources of matter processed by H fusion at $\sim 7.5 \times 10^7$ K, which is enriched in elements, like N and Na, seen to pollute N-enriched nebulae at moderate redshift ($z = 2.4$: Pascale et al. 2023 and Pascale & Dai

2024) and high redshift ($z = 9.4$: Schaerer et al. 2024; $z = 8.3$: Navarro-Carrera et al. 2024; $z = 8.7$ and others: Marques-Chaves et al. 2024). Topping et al. (2024) infer that N-enriched nebulae are common in a large sample at $z > 4$. Indeed, there is evidence that the distinct features of very massive stars, such as strong He II emission, are prominent in the spectra of some young starburst clusters (Vink 2023; Smith et al. 2023). Upadhyaya et al. (2024) present evidence that very massive stars are over-represented in 13 systems between $z = 2.2$ and $z = 3.6$. Similarly, Cameron et al. (2023) determine that stars with $m_* > 50M_\odot$ must be strongly overabundant to explain two-photon emission in nebular-dominated galaxies at $z = 5.9$ and $z = 7.9$. Some of these may be examples of globular cluster formation, considering that the most massive globulars harbor secondary stellar populations enriched in N and other hot burning products (Gratton et al. 2012).

These phenomena bespeak the formation of a top-heavy IMF, either because the high-mass slope flattens (e.g., $\alpha_{\text{high}} < 2$) or because the peak mass or upper mass limit shifts upward, or some combination of these. At the same time, the IMF may become bottom-light: Strader et al. (2011) and Baumgardt et al. (2023) infer that Galactic globular clusters formed a dearth of relatively low-mass stars.

Because massive globular clusters are expected to form in one or more intense bursts, under extreme conditions in terms of the column density Σ , velocity dispersion σ , and other parameters, it is logical to ask how these conditions might lead to the over-production of massive stars. Dib (2023) argues that this could be the

consequence of collisions between molecular cores in the high- Σ environment. Chabrier & Dumond (2024), considering the Central Molecular Zone, attribute the flatter IMF to an impulsive injection of turbulence within the theoretical framework of Hennebelle & Chabrier (2013). We, in contrast, will examine the thermal evolution of these extreme events and ask what implications it has for the stellar mass distribution.

We will focus on conditions representative of massive globular cluster formation, involving systems with total mass $M = 10^6 M_6 M_\odot$ and column density $\Sigma = \Sigma_{\text{cgs}} \text{ g cm}^{-2}$ where M_6 and Σ_{cgs} are both of order unity or greater. We note that the Milky Way globular clusters compiled in the 2010 edition of the Harris (1996) catalog have half-light radii of several pc nearly independently of mass, indicative of $\Sigma_{\text{cgs}} \sim 3M_6$ within that radius. Because of the internal and tidal dynamical interactions that affect cluster evolution (e.g., Marks & Kroupa 2010) this may not faithfully represent the birth conditions, which presumably had higher M and Σ . An upper bound comes from Hopkins et al. (2010), who find $\Sigma_{\text{cgs}} \leq 20$ for all known stellar systems.

Considering only large values of M and Σ simplifies our analysis in two ways. First, as the mean hydrogen density is $10^{4.1} \Sigma_{\text{cgs}}^{3/2} M_6^{-1/2} \text{ cm}^{-3}$ and the H density of a sonic core (see §4) is $\sim 10^{6.8} \Sigma_{\text{cgs}}^2 \text{ cm}^{-3}$, gas and dust are likely to be strongly thermally coupled (Goldsmith 2001). (We examine the conditions for thermal coupling in §8.3.) So long as they are, we can use the dust temperature estimated from radiative transfer as a proxy for the gas temperature, rather than addressing the details of heating and cooling that are critical for analyses of IMF formation in more typical environments (e.g., Elmegreen et al. 2008).

Second, the high columns and velocity dispersions ($\sigma = 10.3 \alpha_{\text{vir}}^{1/2} M_6^{1/4} \Sigma_{\text{cgs}}^{1/4} \text{ km s}^{-1}$, where $\alpha_{\text{vir}} = 5\sigma^2 R/GM$ is the Bertoldi & McKee 1992 virial parameter) imply that most channels of stellar feedback – protostellar outflows, photo-ionized gas pressure, shocked stellar wind pressure, direct starlight momentum, and supernovae – will fail to affect motions on scale of the region (see Fall et al. 2010, Matzner & Jumper 2015, and Menon et al. 2024, for instance). For this reason we will only consider protostellar outflows insofar as they affect the sub-regions that collapse into individual stellar systems and subgroups. On the cloud scale, the only relevant mode of dynamical feedback involves radiation pressure gradient, which in §2 we encapsulate in terms of the Eddington ratio.

1.1. The fundamental mass scale and stellar evolution

A central touchstone for our study of the origin of stellar masses is the *fundamental mass scale*

$$m_{\text{P1}}^3 / \hat{\mu}^2$$

in which $m_{\text{P1}} = (c\hbar/G)^{1/2}$ is the Planck mass and $\hat{\mu}$ is the relevant mass per particle. In practice $\hat{\mu}$ is within a factor of a few of the proton mass m_p , and so the fundamental scale is within an order of magnitude of $m_{\text{P1}}^3 / m_p^2 = 1.85 M_\odot$.

All of the critical mass scales in stellar evolution are cousins of the fundamental scale. These include the mass limits for steady [D or H] burning,

$$\begin{aligned} [m_{*D}, m_{*H}] &\simeq 2.8 \left(\frac{\mu_{*e}}{m_e} \frac{\Psi_{*[D,H]}}{c^2} \right)^{3/4} \frac{m_{\text{P1}}^3}{\mu_{*e}^2} \\ &= [0.02, 0.08] M_\odot, \end{aligned}$$

Chandrasekhar’s (1931) limiting mass of a white dwarf,

$$m_{\text{Ch}} = 3.10 m_{\text{P1}}^3 / \mu_e^2 \simeq 1.43 M_\odot,$$

and the stellar mass for which radiation and gas pressures are equal, which in Eddington’s (1920) standard model is

$$m_{*\text{rad}} = 27.5 m_{\text{P1}}^3 / \mu_*^2 \simeq 140 M_\odot.$$

The evaluation assumes cosmic composition. Note that a star’s diffusive luminosity approaches Eddington’s limit $L_{*\text{Edd}} = 4\pi G m_* c / \kappa_{\text{es}}$ for stellar masses $m_* > m_{*\text{rad}}$.

(In the expressions above, $\mu_* \simeq 4m_p / (3 + 5X) \simeq 0.6m_p$ is the mean molecular weight, and $\mu_{*e} \simeq 2m_p / (1 + X) \simeq 1.17m_p$ is the mass per electron, within a star of hydrogen mass fraction $X \simeq 0.7$; $\mu_e \simeq 2m_p$ is the mass per electron in a white dwarf, $[\Psi_{*D}, \Psi_{*H}] \simeq GM / ([5, 0.8] R_\odot)$ is the gravitational potential depth at the surface of a fully convective star that stably burns [D or H] in its core, and $\kappa_{\text{es}} = 0.2(1 + X) \text{ cm}^2 \text{ g}^{-1}$ is the stellar electron scattering opacity. Coulomb corrections are neglected.)

The formulae for m_{*D} , m_{*H} , and m_{Ch} include \hbar and μ_e because of the importance of electron degeneracy, and c because of the normalization of $\Psi_{*[D,H]}$ (in the burning limits) or because the electrons are relativistic (in Chandrasekhar’s limit).

It is worth commenting on how the fundamental mass arises in $m_{*\text{rad}}$. Here the hydrostatic pressure ($\sim GM^2/R^4$) is balanced in equal parts by radiation pressure ($\sim (kT)^4 / (\hbar c)^3$) and gas pressure ($\sim M kT / \mu R^3$). The coincidence of these pressures sets $M \sim m_{\text{P1}}^3 / \mu^2$, with a numerical prefactor determined by the gas-radiation pressure ratio and the polytropic structure.

A similar situation arises in star formation, when radiation dynamics combine with gas pressure to set a critical mass. In the prototypical example, Rees (1976) has shown that the minimum Jeans mass in a fragmenting cloud is related to the fundamental mass scale of molecular gas, with a prefactor that accounts for the temperature of the environment and aspects of radiative transfer (see §3). We are especially interested in

the possibility that other mass scales, such as the IMF peak (the maximum of $m_*\psi \propto d\dot{N}_*/d\log m_*$) and the upper mass cutoff, are also related to the fundamental mass. As we shall see, these questions are especially pertinent to globular cluster formation.

2. INGREDIENTS

To begin, we gather a few useful ingredients: a simplified radiation transfer solution, an estimate of the relevant luminosities and opacities that enter the radiation transfer calculation, and a rule for extrapolating turbulent motions to small scales.

To highlight the analytical limits for the radiative transfer problem, we adopt a simplified model for the dust temperature distribution $T(r)$ arising due to the reprocessing by dust of a stellar luminosity $L(r)$ within a region of radius r that is optically thick to starlight:

$$T^4 = \frac{L(r)}{\pi r^2 a_r c} f(\tau), \quad (1)$$

where $a_r = \pi^2 k^4 / 15 \hbar^3 c^3$ is the radiation constant and

$$f(\tau) \rightarrow \begin{cases} 1/\tau & \tau \ll 1 \\ \tau/\phi_\tau & \tau \gg 1 \end{cases} \quad (2)$$

where

$$\tau(r) = \kappa(T) f_g \Sigma(r) \quad (3)$$

is the thermal optical depth at r . Here $\Sigma(r) = M(r)/\pi r^2$ is the mean column and $f_g = 1 - f_*$ is the gas fraction. An analysis based on the diffusion approximation within a spherical power law density profile $\rho \propto r^{-k_\rho}$ indicates $\phi_\tau^{1/4} \simeq [(16/3)(5 - k_\rho)/(3 - k_\rho)]^{1/4} \simeq 1.63$ for representative density slopes $1 < k_\rho < 2$.

For the sake of clarity, except in §8.2 we shall define the thick and thin limits of each expression of interest, rather than introducing an interpolating function or some more accurate treatment. Equation (1) is implicit, because the relevant opacity κ depends on T and τ . To be specific, for the optically thin and thick limits we use the Planck and Rosseland means, κ_{P1} and κ_R , respectively. Numerically, we adopt the values computed by [Semenov et al. \(2003\)](#) for composite-aggregate grains. We fit $\kappa_{P1} \simeq 6.1 \delta_{\text{gr}} (T/100 \text{ K})^{1.58} \text{ cm}^2 \text{ g}^{-1}$ and $\kappa_R \simeq 3.0 \delta_{\text{gr}} (T/100 \text{ K})^{1.93} \text{ cm}^2 \text{ g}^{-1}$, respectively, for $T < 150 \text{ K}$, and $(\kappa_{P1}, \kappa_R) \simeq (11.6, 6.6) \delta_{\text{gr}} \text{ cm}^2 \text{ g}^{-1}$ for $150 < T < 400 \text{ K}$. The relative grain abundance δ_{gr} reflects the metallicity in the regime of interest: $\delta_{\text{gr}} \simeq Z/Z_\odot$. We assume $T < 150 \text{ K}$ for most of this work, but consider higher temperatures in §8.

With these evaluations, equation (1) is an interpretable approximation to the multi-frequency radiation transport solution, for which [Chakrabarti & McKee \(2005\)](#) present more accurate and complicated solutions in spherical symmetry. Equation (1) ignores the fact that the radiation field tends to reflect higher temperatures than the local dust temperature, which makes

our evaluation of κ an underestimate. It also neglects the tendency of radiation to flow around dense regions within a clumpy dust distribution. These corrections are likely to act in opposite ways.

For the luminosity L we consider three scenarios, avoiding the regime in which rapid accretion causes the star to swell in size ([Palla & Stahler 1990](#)). First, for an individual low-mass star with $m_* < M_\odot$ accreting at a rate \dot{m}_* , we are interested in the low- \dot{m}_* regime in which deuterium burning sets the gravitational potential, so that $L_* \simeq \Psi_{*D} \dot{m}_*$. Second, for an individual massive star with $M > 10 M_\odot$ we assume L_* limits to the zero-age main sequence (ZAMS) luminosity. We can either evaluate this from stellar models (e.g., [Tout et al. 1996](#)) or approximate it using the radiative diffusion luminosity in Eddington's standard model, in which

$$\frac{\Gamma_*^{1/2}}{(1 - \Gamma_*)^2} = \frac{2^{3/2} m_*}{m_{*,\text{rad}}} \quad (4)$$

implying $\Gamma_* \rightarrow 1$ for $m_* \gg m_{*,\text{rad}}$. Here

$$\Gamma = \frac{L}{L_{\text{edd}}} = \frac{\kappa L}{4\pi G M c} \quad (5)$$

is the Eddington ratio and Γ_* is its value within a massive star, where $(L, M, \kappa) = (L_*, m_*, \kappa_{\text{es}})$. Finally, for a stellar population with total stellar mass $M_* = f_* M$, assuming none of the stars have evolved, we consider $(L/M)_*$ to be of order the IMF-averaged ZAMS value.

The Eddington factor of the cluster-forming cloud is

$$\Gamma = f_* \left(\frac{L}{M} \right)_{*,3} \frac{\kappa_{\text{cgs}}}{13} \quad (6)$$

where $(L/M)_* = 10^3 (L/M)_{*,3} L_\odot / M_\odot$ and 'cgs' means evaluated in those units, so $\kappa = \kappa_{\text{cgs}} \text{ cm}^2 \text{ g}^{-1}$ and $\Sigma = \Sigma_{\text{cgs}} \text{ g cm}^{-2}$. Evaluating equation (1), our choices imply a characteristic temperature for the entire region,

$$T \simeq 61 \text{ K} \times \begin{cases} [\Gamma / (\delta_{\text{gr}}^2 f_g)]^{0.14} & \tau < 1 \\ \Gamma^{1/4} f_g^{1/4} \Sigma_{\text{cgs}}^{1/2} & \tau > 1 \end{cases} \quad (7)$$

$$\rightarrow \begin{cases} 47 [f_* (L/M)_{*,3} / (f_g \delta_{\text{gr}})]^{0.18} \text{ K} & \tau < 1 \\ 58 [f_* f_g \delta_{\text{gr}} (L/M)_{*,3}]^{0.48} (\Sigma_{\text{cgs}}/3)^{0.96} \text{ K}, & \tau > 1 \end{cases}$$

so long as these give $T < 150 \text{ K}$ (for the fits to κ to be valid) and $\Gamma \lesssim 1$ (for dynamical stability).

With this temperature, the self-consistent optical depth can be written $\tau \simeq \{\Sigma / \Sigma_{\text{tr}}, (\Sigma / \Sigma_{\text{tr}})^{2.86}\}$ for optically {thin, thick} regions, where in each regime,

$$\Sigma_{\text{tr}} = \begin{cases} \frac{1.1 \text{ g cm}^{-2}}{[(f_g/0.5) \delta_{\text{gr}}]^{0.71} [(f_*/0.5) (L/M)_{*,3}]^{0.28}} & \tau < 1 \\ \frac{4.0 \text{ g cm}^{-2}}{[(f_g/0.5) \delta_{\text{gr}}]^{0.67} [(f_*/0.5) (L/M)_{*,3}]^{0.32}} & \tau > 1 \end{cases}$$

From this, we see that $(L/M)_{*,3}^{0.3} \delta_{\text{gr}}^{0.7} \Sigma_{\text{cgs}} \simeq 2$ divides optically thick and thin regions halfway through the star

formation process (when $f_g = f_* = 0.5$), although the transition is not sharp: it extends a factor of two on either side of this boundary.

The Eddington factor Γ provides an important dynamical limit on the luminosity-to-mass ratio, as explored by Crocker et al. (2018a). It represents the ratio of between the outward force of radiation and the inward force of gravity on the dusty gas; in the optically thin case, this is equivalent to the ratio of radiation and hydrostatic pressure gradients. Gas is rapidly expelled when $\Gamma > 1$. In fact, dynamically-important magnetic fields are likely to reduce the critical value of Γ , while inhomogeneities may allow matter to persist in high-column concentrations even as low-column regions are blown away.

To actually achieve radiation-driven blowout from an optically thick cloud, a top-heavy IMF is required. In a normal Kroupa (2001) or Chabrier (2005) IMF with a $120 M_\odot$ cutoff, the ZAMS luminosity is $(L/M)_{*,3} \simeq 1$; and as $f_* < 1$ and $\kappa_{R,\text{cgs}} \lesssim 6.6\delta_{\text{gr}} \text{cm}^2 \text{g}^{-1}$, this implies $\Gamma \leq 0.51$ in equation (6). On the other hand, top-heavy IMFs are significantly more luminous; changing (only) the high-mass slope to $\alpha = (2.0, 1.8)$ leads to $(L/M)_{*,3} \simeq (2.3, 3.3)$. Increasing the peak of the IMF also leads to a more luminous population, as does raising the upper mass limit (especially if $\alpha < 2$). Individual stars have have $(L/M)_{*,3} \simeq 65\Gamma_*/(1+X)$ with $\Gamma_* \gtrsim 0.5$ for $m > m_{*\text{rad}}$, which means that sufficiently top-heavy young populations can achieve $\Gamma > 1$. (Note that Menon et al. 2024 have recently studied the consequences of a top-heavy IMF for stellar feedback.)

In the extrapolation of non-thermal turbulent velocities from the cloud scale to the sonic length, we adopt the standard scaling $\sigma_{\text{NT}}(r) = \sigma_c(r/R_c)^\eta$ and assume $\eta \simeq \frac{1}{2}$ in the supersonic regime (Mach number $\mathcal{M} \geq 1$). This is a simplifying idealization of what is actually a complicated and intermittent turbulent velocity field.

A final ingredient is the critical state of a thermally supported object. For an isothermal sphere the critical mass per unit radius is $2.4c_s^2/G$ (Ebert 1955; Bonnor 1956); likewise, for an isothermal filament the critical mass per unit length is $2c_s^2/G$ (Ostriker 1964), where $c_s = \sqrt{kT/\mu}$ is the isothermal sound speed and $\mu = 2.3m_p$ is the mean molecular weight of molecular material. When non-thermal support is relevant, we adjust these formulae by replacing c_s with an effective sound speed c_{eff} that ideally accounts for turbulent and magnetic energy. For simplicity, in evaluating critical masses we ignore the energy in static and perturbed (McKee & Zweibel 1995) magnetic fields, adopting $c_{\text{eff}}^2 \simeq \sigma^2 = c_s^2 + \sigma_{\text{NT}}^2$ where σ is the total line width.

3. OPACITY-LIMITED FRAGMENT MASS

During collapse and fragmentation, the minimum mass of a fragment is the so-called opacity limit (Low &

Lynden-Bell 1976; Rees 1976):

$$m_{\text{opac}} \simeq \left(\frac{c_s}{f_r c}\right)^{1/2} \frac{m_{\text{Pl}}^3}{\mu^2} \quad (8)$$

$$\rightarrow 0.073 M_\odot \begin{cases} \delta_{\text{gr}}^{0.09} [(L/M)_{*,3} f_*/f_g]^{0.24} & \tau < 1 \\ \delta_{\text{gr}}^{1.0} [(L/M)_{*,3} f_* f_g]^{0.71} \left(\frac{\Sigma_{\text{cgs}}}{3}\right)^{1.43} & \tau > 1. \end{cases}$$

where $f_r \leq 1$ is the radiative efficiency, which is determined by radiation diffusion in the regime of interest. Accordingly we set $f_r = 1/q\tau_{\text{opac}}$ where $\tau_{\text{opac}} = \kappa(T)m_{\text{opac}}/\pi r_{\text{opac}}^2$ is the self-consistent optical depth. In the evaluation we set $q^{1/3} = 13.5$ to match equation (26) of Masunaga & Inutsuka (1999).

4. SONIC MASS

The peak of the IMF is likely to originate in marginally stable objects at the sonic scale: those with initial radius $r_s = [c_s/\sigma_{\text{NT}}(R)]^{1/\eta} R$, the value for which turbulent motions match the thermal sound speed (Vázquez-Semadeni et al. 2003; Guszejnov & Hopkins 2015). For a sonic core $\sigma_{\text{NT}}(r_s) = c_s$ so that $c_{\text{eff}}^2 \simeq 2c_s^2$; the core mass is therefore

$$m_s \simeq 4.8 \frac{c_s^2}{G} r_s = 0.96 \frac{\alpha_{\text{vir}}}{\mathcal{M}^{2+1/\eta}} M = 7.6 \frac{c_s^4 \mathcal{M}^{2-1/\eta}}{\alpha_{\text{vir}} G^2 \Sigma} \quad (9)$$

where $\mathcal{M} = \sigma_{\text{NT}}/c_s$ is the Mach number of the environment, evaluated at the local sound speed c_s . We assume $\eta = 1/2$ for the rest of this section, but other values can be accommodated by applying the factor $\mathcal{M}^{1/\eta-2}$. Using equation (1) along with the definition of Γ , we find that

$$m_s \simeq 12.6 \frac{\sqrt{f_g \Gamma}}{\alpha_{\text{vir}}} \frac{m_{\text{Pl}}^3}{\mu^2} \times \begin{cases} 2.66/\tau, & \tau < 1 \\ 1 & \tau > 1. \end{cases} \quad (10)$$

We see that when a cloud is in a particular state – when it is (1) translucent or optically thick ($\tau \gtrsim 1$), (2) at or near the Eddington limit ($\Gamma \lesssim 1$), and (3) suffused with turbulence at or near the spectral slope of Burgers turbulence ($\eta \simeq 1/2$) – all three of which are likely to be satisfied during intense episodes of massive star cluster formation – then its sonic mass will be anchored to a few times the fundamental mass scale for molecular gas,

$$\frac{m_{\text{Pl}}^3}{\mu^2} = 0.34 M_\odot.$$

This is a primary conclusion of our work.

To be specific, we note that for $\Gamma = \alpha_{\text{vir}} = 1$, $m_s \rightarrow 3.1(f_g/0.5)^{1/2} M_\odot$ in the optically thick limit. We expect Γ to saturate at a value less than unity, either because of dynamical effects other than radiation pressure, or because of roughly constant opacity for temperatures above 150 K (see § 8), so the maximal value of m_s in the optically thick regime is likely to be less than $\sim 3 M_\odot$.

With $\eta = 1/2$, thermal cores have a column density comparable to their environment ($\Sigma_s = m_s/\pi r_s^2 = 0.96\alpha_{\text{vir}}\Sigma$). Their optical depths are therefore comparable (if the dust temperature matches the environment) or somewhat greater (if they are warmed from within by a forming star) to that of the environment.

These two possibilities imply two rules for the sonic mass. If the temperature is set by the environment (and $T < 150$ K) one finds,

$$m_{s,\text{env}} \simeq \begin{cases} \frac{0.78}{\alpha_{\text{vir}}} \left(\frac{\Sigma_{\text{cgs}}}{3}\right)^{-1} \left[\frac{f_*(L/M)_{*,3}}{f_g \delta_{\text{gr}}}\right]^{0.36} M_\odot & \tau < 1 \\ \frac{1.22}{\alpha_{\text{vir}}} \left(\frac{\Sigma_{\text{cgs}}}{3}\right)^{0.93} [f_* f_g \delta_{\text{gr}} (L/M)_{*,3}]^{0.97} M_\odot & \tau > 1 \end{cases} \quad (11)$$

where all the parameters refer to the parent cloud. (In formulae like this we assume $T < 150$ K and we do not explicitly impose $\Gamma < 1$; these are additional constraints.)

On the other hand, if the thermal core is heated¹ by the luminosity of an accreting protostar ($L_* \simeq \Psi_{*D} \dot{m}_*$), then its mass is tied to the fundamental constants that set Ψ_{*D} (Krumholz 2011). One must determine the local value of c_s self-consistently with the accretion rate $\dot{m}_* \simeq c_{\text{eff}}^3/G = 2^{3/2}c_s^3/G$. Doing this, we obtain

$$m_{s,\text{self}} \simeq \begin{cases} 0.56 \delta_{\text{gr}}^{-0.33} [\alpha_{\text{vir}}(\Sigma_{\text{cgs}}/3)]^{-0.67} M_\odot & \tau_s < 1 \\ 0.47 \delta_{\text{gr}}^{0.78} [\alpha_{\text{vir}}(\Sigma_{\text{cgs}}/3)]^{1.33} M_\odot & \tau_s > 1 \end{cases} \quad (12)$$

where τ_s is the optical depth of the self-irradiated core; self-consistently $\tau_s > 1$ when $\alpha_{\text{vir}} \Sigma_{\text{cgs}} \delta_{\text{gr}}^{1/2} \gtrsim 4.2$. Comparing this estimate of $m_{s,\text{self}}$ to the environmentally-heated value $m_{s,\text{env}}$, and accounting for details like the fact that optically-thin cores can only exist within optically-thin environments, suggests that self-heating by accretion luminosity is important either for environments that are not particularly luminous ($f_*(L/M)_{*,3} < 1$) or for regions of high column density in which the core is optically thick to its accretion luminosity.

However, the last conclusion is unlikely to be valid because there is (quite literally) a hole in the logic leading to the optically thick branch of equation (12): it follows from the diffusion approximation in spherical symmetry, and does not account for a protostellar outflow cavity. An outflow cavity strongly modifies the problem of radiation diffusion in the thick limit, by providing an optically thin escape path for protostellar radiation (Krumholz et al. 2004; Matzner & Levin 2005). While detailed analysis is in order (along the lines of Robitaille 2017), we can roughly account for this effect by setting

$f(\tau) \simeq 1$ in equation (1). This gives the modified optically thick solution

$$m_{s,\text{self}} \simeq 1.0 [\alpha_{\text{vir}}(\Sigma_{\text{cgs}}/3)]^{-1/9} M_\odot \quad \tau_s > 1 \quad (13)$$

which both highly insensitive to the environment, and consistently lower than the result for a core heated by an optically-thick environment (equation 11) – except for especially low values of the combination $f_g g_* \delta_{\text{gr}} \Sigma (L/M)_*$, which are unlikely to be consistent with $\tau > 1$ in any case.

Based on this, we tentatively conclude that the sonic mass scale is self-consistently determined by the surrounding radiation environment in the context of intense stellar cluster formation, whereas internal accretion luminosity is the relevant heating source in contexts more like well-studied Galactic environments.

5. UPPER MASS SCALE

Between m_s and the cloud mass M , the only physical effect clearly associated with a mass scale has to do with the stellar luminosity: Γ_* approaches unity as m_* exceeds $m_{*,\text{rad}} = 140 M_\odot$. Note that an optically thick dusty region that is bound by the gravity of a single massive star has $\Gamma_{\text{cl}} \simeq 13 \delta_{\text{gr}} \Gamma_*$. Using Equation 4, this means that some critical value of Γ_{cl} (such as unity) can be associated with a value of m_* so long as $\delta_{\text{gr}} \gtrsim \Gamma_{\text{cl,crit}}/13$. The stellar upper mass limit is likely to be related to $m_{*,\text{rad}}$ either as a result of the stars' own stability and wind production (due to high Eddington factors and radiation pressure support), or due to the super-Eddington nature of stellar accretion in dusty gas (if the metallicity is not too low). Indeed, numerical experiments with sufficiently low metallicity to achieve $\Gamma_{\text{cl}} < 1$ around very massive stars do find that these continue to accrete well above $m_{*,\text{rad}}$ (M. Grudić, private communication, 2024).

5.1. Stabilization of massive-star accretion flows

Massive stars (or star systems) grow from regions that encompass many sonic masses, which makes them sensitive to the stability of the regions that feed them. The more stable the feeding zone, the more successfully a growing massive star can accumulate gas (rather than companions). Our analysis of this will be similar to that of Krumholz & McKee (2008), except that we assume the region is significantly heated by starlight.

As accretion tends to occur along dense filaments, and as the critical mass per unit length λ of a thermally-supported filament is $\lambda_{\text{th}} = 2c_s^2/G$, we conclude that the character of the accretion flow is determined by the stability parameter

$$\zeta_{\text{fil}} = \frac{2c_s(r)^2 r}{GM(r)} = \frac{2}{5} \frac{\alpha_{\text{vir}}(r)}{\mathcal{M}(r)^2}, \quad (14)$$

¹ Hennebelle et al. (2020) argue that the protostellar luminosity problem (Kenyon et al. 1990) is evidence that protostellar heating is ineffective. However, Offner & McKee (2011) find that accelerating and unsteady accretion suffices to resolve the problem, which leaves open the possibility that a sonic core can regulate its own mass.

which we can evaluate using equation (9) as

$$\zeta_{\text{fil}} = \frac{2}{5} \alpha_{\text{vir}} \left(\frac{m_s}{0.96 \alpha_{\text{vir}} M} \right)^{\frac{2\eta}{2\eta+1}} \quad (15)$$

$$\xrightarrow{\eta=1/2} \left(\frac{\alpha_{\text{vir}} m_s}{6.0 M} \right)^{1/2}.$$

We envision that the collapsing accretion zone, with mass distribution $M(r)$, contains a range of filamentary structures with values of λ distributed around the characteristic value $M(r)/r$ in a manner determined by the physical effects at play (Klassen et al. 2017) – and that the fraction of this region capable of accreting before it undergoes fragmentation depends on the combination $\lambda_{\text{th}} r / M(r) = \zeta_{\text{fil}}$. If accretion involves a number of filaments N_{fil} that exceeds $1/\zeta_{\text{fil}}$, it is possible for the accretion flow to be completely stabilized by thermal pressure alone (see Matzner & Jumper 2015).

Turbulent motions, magnetic fields (Fiege & Pudritz 2000), and tidal gravity (Lee & Hennebelle 2018) also stabilize the region. Unlike these, the thermal support parameterized by ζ_{fil} is clearly a function of the star formation activity and radiative transfer, rather than dimensionless properties of the initial conditions. (The same might be said for non-ideal magnetic effects, but these lie beyond the scope of our work.)

Equation (15) indicates that the stability of an accretion zone depends on the number of thermal core masses it contains, which in turn reflects the radiation environment. Effects that increase m_s also enhance the stability of accretion. And, just as a thermal core can be self- or environmentally-heated, a massive star’s accretion zone can be heated and stabilized either by the star itself, or by the radiation environment of its parent region. We stress that the accretion flow can feed a growing stellar system or sub-cluster as opposed to a single star (Kratte & Matzner 2006, Kratte et al. 2010, Matzner & Jumper 2015), and stabilization provides a path to flatten the high-mass slope of the IMF as seen in simulations by Krumholz et al. (2011), Commerçon et al. (2011), and Myers et al. (2013). It also provides an explanation for primordial mass segregation in optically-thick cluster environments; we note that Baumgardt et al. (2008) present evidence for primordial segregation in globular clusters. We return to this point in § 8.1.

6. DYNAMICAL INFLUENCE OF PROTOSTELLAR OUTFLOWS

We previously considered the possibility that protostellar outflows will affect the ability of accreting protostars to set their own accretion reservoir. Now let us consider the role of protostellar winds and jets in returning matter to the environment, a process that limits the efficiency of individual or clustered star formation (Matzner & McKee 2000, hereafter MM00). We assume that the outflow momentum per stellar mass, denoted

$f_w v_w$ for consistency with MM00, is related to the stellar Keplerian speed $\Psi_*^{1/2}$ by a factor $\phi_w \simeq 0.1 - 0.2$ that accounts for the ratio of wind to accreted matter as well as the ratio of wind speed to Keplerian speed. That is,

$$f_w v_w = \phi_w \Psi_*^{1/2}. \quad (16)$$

Using this, we can obtain MM00’s parameter X (their eq. 3, in which $c_g \ln 2 / \theta_0 \simeq 5.8$) and the single-star formation efficiency ε (their eq. 31, for spherical cores, or eq. 44, for flattened cores) or larger regions (their eq. 55).

To evaluate ε for thermal cores of the sonic mass, we take $\Psi_*^{1/2} = \Psi_{*D}^{1/2} = 195 \text{ km s}^{-1}$, and we ignore the possibility that the core is flattened (or more likely, elongated but misaligned from the outflow axis). The escape velocity of such a core is $v_{\text{esc},s} \simeq 3.1 c_s$, according to the rule $m_s / r_s \simeq 4.8 c_s^2 / G$. For the case of an environmentally-heated core we can evaluate c_s from equation (7) to obtain

$$X \simeq \frac{0.44}{\phi_w / 0.1} \times \begin{cases} (\Gamma / f_g)^{0.07} \delta_{\text{gr}}^{-0.14} & \tau < 1 \\ (\Gamma f_g \Sigma_{\text{cgs}}^2)^{1/8} & \tau > 1 \end{cases} \quad (17)$$

for stars forming within regions of mass $m_{s,\text{env}}$, from which (neglecting the small wind mass correction in MM00 eq. 31)

$$\varepsilon = \frac{2X}{1 + \sqrt{1 + (2X)^2}} \simeq X(1 - X^2) \quad (18)$$

where the approximation is valid to 10% for $X < 0.5$.

We see that environmentally-heated thermal cores form stars at about 38% efficiency according to this estimate. (It is possible but not certain that smaller cores, even down to m_{opac} , might develop outflows and form at a similar efficiency.) Self-heated cores would form at moderately higher efficiency, thanks to their elevated temperatures.

For massive star formation, a couple factors are different. First, the stellar potential well of a massive star is deeper. Second, the relevant escape velocity reflects the entire accretion zone, which might feed more than a single object, and this region is not thermally supported. Together, we find that

$$X \simeq \frac{0.42}{\phi_w / 0.1} \frac{\Psi_{*H}^{1/2}}{\Psi_*^{1/2}} \left(\frac{M}{m_{*,\text{rad}} \Sigma_{\text{cgs}}} \right)^{1/4} \quad (19)$$

for massive stars within their accretion regions (normalizing M to the stellar mass scale $m_{*,\text{rad}} = 140 M_\odot$, and Ψ_* to the value defined earlier for H-burning convective stars). This indicates that individual massive stars can remove a significant amount of matter from their accretion environments, and form with an outflow-limited efficiency very similar to that of individual low-mass stars.

There may exist stars that form at higher efficiency, because of the reduction in Ψ_* associated with an inflated protostellar radius, but we do not attempt to calculate this effect.

7. INFLUENCE OF BINARY AND MULTIPLE FORMATION

Another key factor affecting the numbers and masses of stars, relative to a thermal scale such as m_s , is the fragmentation into binary or multiple star systems. This is obviously important for the lower IMF, insofar as heat from starlight and viscous dissipation is critical to stifling the fragmentation of protostellar disks into large numbers of brown dwarfs (Matzner & Levin 2005; Bate 2009; Stamatellos & Whitworth 2009; Offner et al. 2009; Urban et al. 2010). At somewhat higher masses, fragmentation will tend to suppress the IMF peak mass by some factor $\phi_{\text{mult}} \sim 0.5$, as the observed companion frequency is of order 0.6 around $1M_\odot$ (and strongly correlated with the mass of the primary, at least for local stellar populations; see Offner et al. 2023).

We wish to infer how ϕ_{mult} is likely to depend on environmental factors. Our strategy will be to evaluate the specific angular momentum j_s of a sonic core, assume some fraction of this is not lost to magnetic braking during star formation, and then examine the gravitational stability of the structure (such as an accretion disk) that results. In this we follow Matzner & Levin (2005), Kratter & Matzner (2006), and Kratter et al. (2010), hereafter ML05, KM06, and K+10, respectively. Our procedure is designed to capture close binary formation from disk fragmentation, rather than the more stochastic turbulent channel for the formation of wide binaries that is inferred both from simulations (Offner et al. 2010) and observations (Moe et al. 2019; El-Badry & Rix 2019).

For a sonic core $j_s = \theta_j r_s \sigma_{NT}(r_s) = \theta_j r_s c_s$, where we consider θ_j to be chosen from a Maxwellian distribution peaked around $0.383(\eta/0.5)^{0.49}$. In this we follow KM06's evaluation of the angular momentum contained within an uncorrelated Gaussian-random velocity field with line width-size index η , when integrated over the density structure of a critical Bonnor-Ebert sphere in the manner of Burkert & Bodenheimer (2000). Assuming a fraction f_j of the angular momentum survives magnetic braking to form stellar system with mass $m_s/\varepsilon = 4.8c_s^2 r_s/\varepsilon G$ this implies an orbital radius of about $r_s f_j^2/33\varepsilon$, or

$$a_{\text{orb},s} \simeq 107 \frac{f_j^2}{\varepsilon \alpha_{\text{vir}}} \text{AU} \times \begin{cases} [\Gamma/(\delta_{\text{gr}} f_g)]^{0.14} \Sigma_{\text{cgs}}^{-1} & \tau < 1 \\ [f_g \Gamma]^{1/4} \Sigma_{\text{cgs}}^{-1/2} & \tau > 1 \end{cases} \quad (20)$$

$$\rightarrow \begin{cases} 80 \frac{f_j^2}{\varepsilon \alpha_{\text{vir}}} [f_*(L/M)_{*,.3}/(\delta_{\text{gr}} f_g)]^{0.18} \Sigma_{\text{cgs}}^{-1} \text{AU} & \tau < 1 \\ 35 \frac{f_j^2}{\varepsilon \alpha_{\text{vir}}} [\delta_{\text{gr}} f_g f_*(L/M)_{*,.3}]^{0.48} \Sigma_{\text{cgs}}^{-0.03} \text{AU} & \tau > 1 \end{cases}$$

for environmentally-heated cores.

From the system accretion rate \dot{M}_{sys} , system mass M_{sys} , specific angular momentum j , and local (e.g., disk) sound speed c_{sd} one can compute the dimension-

less parameters

$$\xi_d = \frac{G \dot{M}_{\text{sys}}}{c_{sd}^3} \quad \text{and} \quad \Gamma_d = \frac{j^3 \dot{M}_{\text{sys}}}{G^2 M_{\text{sys}}^3}.$$

A disk that forms with these parameters has a characteristic aspect ratio of order $(\Gamma_d/\xi_d)^{1/3}$, as discussed by K+10. In the thin-disk limit $(\Gamma_d/\xi_d)^{1/3} \ll 1$, Toomre's (1964) stability parameter is $Q_d \simeq 3\alpha_d/\xi$ (Gammie 2001), where α_d is an effective viscosity parameter meant to capture transport by the gravitational instability. If we adopt ML05's estimate for the maximal viscosity parameter (which is $\max \alpha_d = 0.23$), we find that sufficiently thin disks should fragment when $\xi \gtrsim 1.12$. However, K+10 show that finite thickness stabilizes accretion, and identify a fragmentation boundary $\xi_d \gtrsim (850\Gamma_d)^{2/5}$ at the finite resolution of their simulations. To be definite, we take

$$\xi_d > \max[1.12, (850\Gamma_d)^{2/5}] \quad (21)$$

as the fragmentation criterion, while acknowledging that both branches of this formula are uncertain.

Applied to a sonic core for which $\dot{M}_{\text{sys}} = \varepsilon c_{\text{eff}}^3/G = 2^{3/2} \varepsilon c_s^3/G$, $M_{\text{sys}} = \varepsilon m_s$, and $j = j_s$, we find $\Gamma_d \simeq (\eta/0.5)^{1.47}/(700\varepsilon^2)$ so that $(850\Gamma_d)^{2/5} = 2.25(\varepsilon/0.4)^{-4/5}$. As this value exceeds 1.12, we take

$$\xi_{d,\text{crit},s} = 2.25(\varepsilon/0.4)^{-4/5}$$

to be the critical value of ξ_d for a sonic core (adopting $\eta = 0.5$ at this point, for simplicity). We note that this implies that fragmentation will occur when the outer disk becomes marginally colder than its parent core.

To determine whether disks do fragment by this criterion, we must compute ξ_d . We assume the outer disk is optically thick; this is reasonable, as the disk column density Σ_d is self-consistently 1.6 to 2 dex higher than that of its parent core, which in turn is comparable to that of the environment.

First, consider a disk warmed by its own internal dissipation, rather than by starlight. Using the logic leading to ML05 eq. (31), we see that the value of ξ_d in such a disk is directly related to its outer orbital frequency. We equate the local cooling rate $4acT_d^4/(3\kappa_d \Sigma_d)$ with the heating rate $3\dot{M}_{\text{sys}} \Omega_d^2/8\pi$, in the context of viscous accretion at the rate $\dot{M}_{\text{sys}} = 3\pi\alpha_d \Sigma_d c_d^2/\Omega_d$. Solving for $\xi_d = G\dot{M}_{\text{sys}}/c_d^3$ and naming the result $\xi_{d,\text{visc}}$, we find

$$\xi_{d,\text{visc}} = \left[\frac{2\alpha_d ac}{3(\kappa_d/T_d^2)} \right]^{1/2} \frac{4\pi G\mu}{k} \Omega_d^{-3/2} = \left(\frac{\Omega_\xi}{\Omega_d} \right)^{3/2} \quad (22)$$

where Ω_d is the orbital frequency of the outer disk, and the period corresponding to $\xi_{d,\text{visc}} = 1$ is

$$\frac{2\pi}{\Omega_\xi} \simeq 500 \left(\frac{\delta_{\text{gr}}}{\alpha_d/0.23} \right)^{1/3} \text{yr}. \quad (23)$$

In this evaluation we assume that the opacity law is unchanged between the core and the disk, so that $\kappa_d/T_d^2 \simeq 3.0 \times 10^{-4} \delta_{\text{gr}} \text{cm}^2 \text{g}^{-1}$ at the relevant temperatures.

Using equation (22), our fragmentation criterion corresponds to disk periods $\gtrsim 860(0.23\delta_{\text{gr}}/\alpha_d)^{1/3}(\eta/0.5)^{0.37}(\varepsilon/0.4)^{-0.53}$ yr, whereas the typical disk periods are a few times longer if all parameters (f_j , Σ_{cgs} , etc.) are taken to be unity. Phrased in terms of the stability parameter ξ_d , the comparison implies

$$\frac{\xi_{d,\text{visc}}}{\xi_{d,\text{crit},s}} \simeq 7.9 \frac{f_j^{9/2} (\alpha_d/0.23)^{1/2}}{\alpha^{3/2} (\varepsilon/0.4)^{11/5}} \times \begin{cases} \frac{(\Gamma/f_g)^{0.10}}{\delta_{\text{gr}}^{0.71} \Sigma_{\text{cgs}}^{3/2}} & \tau < 1 \\ \frac{(f_g \Gamma)^{3/16}}{\delta_{\text{gr}}^{1/2} \Sigma_{\text{cgs}}^{9/8}} & \tau > 1 \end{cases} \quad (24)$$

$$\rightarrow 1.3 \frac{f_j^{9/2} (\alpha_d/0.23)}{\alpha^{3/2} (\varepsilon/0.4)^{11/5}} \times \begin{cases} \frac{[f_* (L/M)_{*,3}/f_g]^{0.13}}{\delta_{\text{gr}}^{0.63} (\Sigma_{\text{cgs}}/3)^{3/2}} & \tau < 1 \\ \frac{[f_g f_* (L/M)_{*,3}]^{0.36}}{\delta_{\text{gr}}^{0.14} (\Sigma_{\text{cgs}}/3)^{0.78}} & \tau > 1 \end{cases}$$

We see that for fiducial parameters, viscous dissipation will not prevent the disk formed from an environmentally-heated sonic core from fragmenting. The removal of mass by protostellar outflows (ε) is a destabilizing factor, as it increases a_{orb} and decreases Ω_d . However, it would take only a mild amount ($f_j \lesssim 0.63$) of magnetic braking to overcome this effect, and make viscous heating more of a barrier to fragmentation.

Considering environmental parameters, we see that fragmentation is suppressed by an increase in the column density of the environment, as cores with higher Σ make smaller and more stable disks. Increasing the metallicity also suppresses fragmentation (through δ_{gr}), primarily because the disk is optically thick. (This implies a metallicity/close-binary anticorrelation like the one discovered by Moe et al. 2019.)

According to equation (24), disks in more luminous regions are less stable because this increases r_s and hence a_{orb} . However, the stabilizing influence of irradiation is not yet included; we turn to this next.

To consider the case where the irradiating source is the star, with $L_* = \Psi_* \dot{M}_{\text{sys}}$, we adopt the model developed by ML05 in which starlight strikes the inner edge of an outflow cavity and then indirectly warms the disk to an equilibrium temperature determined by $acT_{d,\text{irr}}^4 \simeq 0.1\varepsilon^{0.35} L_*/(\pi a_{\text{orb}}^2)$. This leads to a moderate suppression of fragmentation, in that

$$\frac{\xi_{d,\text{irr}}}{\xi_{d,\text{crit},s}} \simeq 0.63 \frac{f_j^{3/2}}{\alpha^{3/4}} \left(\frac{\varepsilon}{0.4}\right)^{0.81} \times \begin{cases} \frac{(\Gamma/f_g)^{0.24}}{\delta_{\text{gr}}^{0.47} \Sigma_{\text{cgs}}^{3/4}} & \tau < 1 \\ (f_g \Gamma)^{0.42} \Sigma_{\text{cgs}}^{0.09} & \tau > 1 \end{cases} \quad (25)$$

Even in the absence of stellar luminosity, a disk will be warmed by its environment. When the environment is optically thick, this implies $c_d \gtrsim c_s$ and therefore $\xi_{d,\text{irr}}/\xi_{d,\text{crit},s} \lesssim 0.5(\varepsilon/0.4)^{9/5}$. (In the optically thin case, environmental irradiation is less stabilizing when

the environment is not as luminous; additional factors like $\Sigma_{\text{cgs}}^{-3/8}$ appear.)

Although we have seen that stellar and environmental irradiation are stabilizing factors, especially for optically thick cores, these estimates are close enough to unity that we do not expect them to entirely shut off binary and multiple star formation on their own. As Offner et al. (2023) stress, fluctuations in the mass accretion rate and central luminosity are likely to provide a route for fragmentation.

Briefly considering self-heated cores, we note that heating by the central object makes a sonic core larger, which increases a_{orb} , which increases the likelihood of fragmentation. As discussed in §4, however, the presence of an outflow cavity is likely to prevent sonic cores from being self-heated in the contexts of interest.

8. DISCUSSION

We have found that the mass scales and modifying factors that affect the stellar mass distribution all depend to some extent on the parameters of the region, but that the dependence is not necessarily monotonic because of the shift from optically thin to optically thick behavior. Relevant factors include the column density and dust content, as well as the light-to-mass ratio of the stellar population. It is also relevant that the Eddington ratio cannot become large, as this fact connects the sonic mass to the fundamental masses of stars.

Important questions arise: How sensitive is the high-mass slope of the IMF (α_{high}) to the environment? In the end, how strongly does the IMF regulate itself in the process of thermal feedback? What limitations arise from our physical and dynamical assumptions? And, how well do our predictions match trends inferred within well-studied globular clusters?

8.1. High-mass slope and primordial segregation

We consider massive stars to be the dominant fragments in sub-regions that collapse from the turbulent background (e.g., Bonnell et al. 2004). In the excursion-set theory of Hopkins (2012a,b), the mass function of collapsing regions is determined by the statistics first barrier crossings, with high-mass slopes like those of giant molecular clouds ($\alpha_{\text{coll}} \simeq 1.7$: Hopkins 2012a eq. 29) while the upper stellar mass function acquires the steeper distribution of second barrier crossings (typically $\alpha_{\text{high}} \simeq 2.35$: Hopkins 2012b eq. 31). The role of sub-fragmentation in steepening α_{high} was also stressed by Oey (2011).

As discussed in §5.1, the tendency of a collapsing region to fragment will depend on its thermal state, as represented by the accretion stability parameter ζ_{fl} . Equation (15) shows that an increase of m_s will tend to suppress fragmentation in the regions that collapse to form massive stars, thereby reducing α_{high} to some degree. If the dependence on m_s is sufficiently strong, it may be

possible for this effect to increase the specific luminosity $(L/M)_*$ enough to achieve $\Gamma > 1$.

To explore this possibility, we entertain a relatively strong realization of this effect, such that $\alpha_{\text{high}} = 2.35$ when $m_{s,\text{env}} \simeq 0.2 M_\odot$ (as in local star formation), flattening to $\alpha_{\text{high}} = 1.75$ when $m_{s,\text{env}} \rightarrow 3.1 M_\odot$ (the saturated value of eq. [10]). This suggests

$$\alpha_{\text{high}} \simeq 2.0 - 0.5 \log_{10}(m_{s,\text{env}}/M_\odot). \quad (26)$$

While this specific form is purely hypothetical, the existence of a positive correlation between m_s and α_{high} is supported by the ability of stellar radiation to inhibit fragmentation in the simulations of [Krumholz et al. \(2011\)](#), [Commerçon et al. \(2011\)](#), and [Myers et al. \(2013\)](#), for instance. Such a correlation also promotes a tendency for higher-column regions to host more massive stars, and for the primordial segregation of massive stars toward the high-column regions within an optically thick clump, as we discuss below. If the correlation is sufficiently strong to generate $(L/M)_{*3} \gtrsim 2$, as equation (26) is, then it can self-consistently lead to $\Gamma \gtrsim 1$ within optically thick regions. This allows for radiation pressure to dynamically regulate star formation (e.g., [Crocker et al. 2018a](#)), as we demonstrate using a toy model in § 8.2.

It is straightforward to see why a positive correlation implies that massive stars form preferentially in the thickest parts of optically thick regions. In the optically thick regime, $m_{s,\text{env}}$ increases nearly linearly with $\delta_{\text{gr}}\Sigma(L/M)_*$ so long as $T < 150$ K (eq. [11]). An increase in $m_{s,\text{env}}$ will raise $(L/M)_*$ to some degree, especially if it causes α_{high} to increase as well. This implies that thick regions higher column densities should display flatter mass functions – and the trend should hold both between regions and within an individual region. In other words, it implies a flattening of the IMF in star clusters of higher initial $(Z/Z_\odot)\Sigma_*$ (among those that are optically thick to begin with), as well a flattening of the IMF toward the high-column portion of a single region. The latter effect amounts to a primordial segregation of massive stars within the region. Note: these phenomena are related to, but somewhat distinct from, the column density threshold proposed by [Krumholz & McKee 2008](#). It is likely that their threshold plays a role in preventing massive star formation in our optically thin regime.

For regions that warm themselves above 150 K, the dust opacity becomes roughly constant, weakening somewhat the sensitivity of $m_{s,\text{env}}$ and α_{high} to the environmental parameters.

8.2. A toy model

A toy model of star cluster formation helps to illustrate some of these interactions, and demonstrate that a relation like equation (26) can lead to dynamically significant radiation pressure. We stress that the toy model presented here is not meant to represent a realistic evolution. We grow a stellar system by holding Σ

artificially fixed, building up the luminosity and mass of a stellar population by evolving from low to high f_* . Ingredients for this include: (i) a piecewise power law model for the [Planck, Rosseland] opacities, $\kappa_{[\text{P},\text{R}]} = [6.1, 3.0]\delta_{\text{gr}} \min(T/100, 1.5)^{[1.93, 1.58]}$; (ii) an estimate of $\tau(T)$, for which we use $(\tau_{\text{P}} + 3\tau_{\text{R}}^4)/(1 + 3\tau_{\text{R}}^3)$, where $\tau_{[\text{P},\text{R}]}$ are the self-consistent [Planck, Rosseland] optical depths given T , $\delta_{\text{gr}}f_g\Sigma$, and $f_*(L/M)_*$; (iii) a self-consistent value of T given $\delta_{\text{gr}}f_g\Sigma$ and $f_*(L/M)_*$, which involves solving equation (1) with $f(\tau) = [\tau_{\text{P}}^{-2} + (\tau_{\text{R}}/\phi_\tau)^2]^{1/2}$; (iv) an estimate of m_{opac} , as the maximum of the options in equation (8); (v) an evaluation of $m_{s,\text{env}}$ using equation (9); (vi) an evaluation of X and ε from equations (17) and (18); and (vii) an estimate of α_{high} , for which we use equation (26).

Given these, we construct at every point in the evolution an instantaneous IMF that has a log-normal section, peaked at $m_{\text{peak}} = \phi_{\text{mult}}\varepsilon m_{s,\text{env}}$ (with ϕ_{mult} fixed at 0.75 for simplicity), has a width of 0.5 dex, and is bounded below by $m_{\text{min}} = m_{\text{opac}}$. This is joined to a high-mass power law of logarithmic slope $-\alpha_{\text{high}}$, in such a way that the IMF and its slope are both continuous. This extends to an upper limit m_{max} , held fixed at $120 M_\odot$ for simplicity. For this IMF the value of $(L/M)_*$ is estimated using the zero-age main sequence luminosity from [Tout et al. \(1996\)](#), which determines dL_*/dM_* as stellar mass is accumulated. This is a simple integration, because we ignore the possibility that there might be time for stellar evolution to change the luminosity of the extant stars.

Figure 1 provides two examples of this toy model, for $\Sigma_{\text{cgs}} = 3$ and $\Sigma_{\text{cgs}} = 20$, in which $\alpha_{\text{vir}} = \delta_{\text{gr}} = 1$. In both cases we start with $f_* = 0.1$ and $(L/M)_{*3} = 1$ and evolve to higher f_* . In both models, the thermal feedback from newborn stars is sufficient to raise m_s and flatten α_{high} to the extent that the Eddington factor becomes significant ($\Gamma > 0.8$, say). As expected, this transition happens earlier in the higher-column example (at $f_* = 0.64$ for $\Sigma_{\text{cgs}} = 20$, compared to $f_* = 0.88$ for $\Sigma_{\text{cgs}} = 3$).

Importantly, we note that the appearance of a super-Eddington state in this model is the direct consequence of the flattening of α_{high} we assumed by adopting equation (26). If instead we fix $\alpha_{\text{high}} = 2.35$, we find that $\Gamma > 0.8$ is not achieved until the gas is almost entirely consumed.

8.3. Regime of validity

A few of the assumptions in this paper limit its regime of validity. First, dust must be sufficiently abundant that the collisions between gas and grains will tightly couple their temperatures within sonic cores. Examining [Omukai \(2000\)](#)'s figure 1, we estimate that the dust and gas temperatures agree within 15% when $n_H > 10^{4.5}(Z/Z_\odot)^{-1.33} \text{ cm}^{-3}$. Noting that the thermal pressure within a sonic core roughly matches the hydrostatic

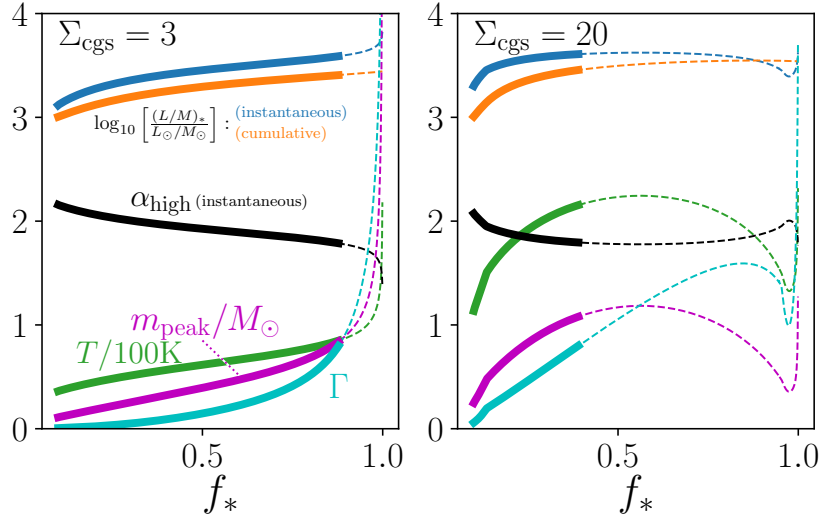


Figure 1. A toy model for star cluster formation, in which Σ is held fixed at either 3 (left) or 20 (right), and the stellar population evolves under the influence of its own radiation while the upper-mass slope evolves according to the hypothetical relation (26). Curves are plotted as dashed lines once the Eddington factor Γ exceeds 0.8, as this is likely to imply disruption by radiation pressure gradients. In the right panel, the kink in the lines arises from the change in the opacity law at $T = 150$ K. See § 8.2 for additional details.

pressure $\sim 0.7f_g G \Sigma^2$ of the environment, and that the density threshold is always reached within the optically thin branch of equation (7), we find that dust and gas are self-consistently coupled whenever

$$\frac{Z}{Z_\odot} \gtrsim 10^{-2.4} \left(\frac{\Sigma_{\text{cgs}}}{3} \right)^{-1.32}. \quad (27)$$

This would include all of the globular clusters in the Harris (1996) catalog, assuming they formed in a compact state with $\Sigma_{\text{cgs}} \gtrsim 3$.

Second, because we have ignored the cosmic background radiation in determining the dust temperature, our results are only valid up to the redshift at which the background temperature $2.725(1+z)$ K approaches the temperature in equation (7). This criterion is most relevant to optically thin environments with high dust content, which are relatively cooler, for which it amounts to

$$z < 17.2 \left[\frac{(L/M)_{*3}(f_g^{-1} - 1)}{\delta_{\text{gr}}} \right]^{0.18} - 1. \quad (28)$$

Third, our dust temperature estimate should be adjusted the clumpy nature of the dust distribution and from incomplete thermalization of the radiation field. Crocker et al. (2018a) use the characteristics of fully developed supersonic turbulence to argue that the impact of inhomogeneities on the transfer of radiation will be relatively minor (their Appendix C), but radiation hydrodynamics solutions can help to calibrate this. Likewise, Monte Carlo transfer solutions will be useful to quantify the impact of a non-thermal radiation field.

Finally, although we have not adopted a specific cluster formation scenario, we have assumed it is rapid enough that no stars leave the main sequence. Also, when estimating τ we assumed significant gas fraction; this is more consistent with the monolithic collapse than extended accretion. The formation of enriched stars from cooled stellar ejecta (Wünsch et al. 2017) or ejecta mixed with ambient material (Lochhaas & Thompson 2017) involves extended accretion, so this assumption may be more appropriate for the first generation than the second one.

8.4. Application to well-studied globular clusters

In our theory, the low-mass IMF should depend primarily on the value of m_s , with secondary modifications from binary fragmentation and outflow ejection. It is interesting to compare this to the apparent IMF variations within globular clusters, bearing in mind that living stars within them have $m_* \lesssim 0.8M_\odot$, and that stellar remnants contribute to the total mass while they linger (e.g., Breen & Heggie 2013). Qualitatively, the relatively large values of m_s implied by equations (11) and (12) are consistent with the inferences of bottom-light IMFs mentioned in § 1. Quantitatively, our finding that $m_{s,\text{env}}$ is approximately $\propto (\delta_{\text{gr}}^{-1/3} \Sigma^{-1}, \delta_{\text{gr}} \Sigma)$ in optically (thin, thick) clouds is only compatible with Strader et al. (2011)’s determination that clusters in M31 are more bottom light at low Z if the low-mass stars in question form in an optically thin region – perhaps in their outskirts. (Note also: Zonoozi et al. (2016) conclude that $Z^{-1/7} \rho_*$ correlates with a bottom-light IMF; however Strader et al. (2011) attribute the variation with ρ_*

to dynamical evolution.) These points warrant further study.

9. CONCLUSIONS

We draw four major conclusions about intense starbursts like those that give rise to massive globular clusters:

1. Important quantities, such as the opacity-limited minimum mass, the sonic mass, the efficiency of individual star formation, the tendency for binary fragmentation, and the high-mass slope of the IMF, can all be related to the radiation environment, which in turn is determined by the transport of stellar radiation through the dusty star-forming environment. Each of these quantities can be approximated analytically in the optically thin or thick cases, although some of the forms proposed here (α_{high} , in particular) are quite speculative.
2. When expressed in terms of the Eddington factor Γ , the sonic mass m_s within an optically thick starburst region is related to the fundamental mass scale composed of the Planck mass and the mean molecular weight. (This was already true of the minimum stellar mass: Rees 1976.) Because this is similar to the fundamental mass scales for stellar evolution, such as Chandrasekhar's limit, it implies that the ultimate production of stellar remnants is not entirely arbitrary. At a basic level, this arises because radiation and gas pressures become comparable within sonic cores.
3. Among regions that are optically thick to their own thermal radiation, a plausible line of argument suggests that the IMF should flatten as the

sonic mass increases, and that this accompanies an increase of the quantity $(Z/Z_{\odot})\Sigma$. This phenomenon is expected to operate among star forming environments and also within them, where it produces a primordial segregation of massive stars in the highest-column substructures.

4. The Eddington factor Γ can become appreciable in the midst of star cluster formation, thanks to the luminosity-to-mass ratio of young stellar populations and the character of dust opacities. In particular, a relatively small flattening of the IMF is sufficient to allow radiation pressure to become dynamically significant. We present a toy model in which this occurs naturally in the process of star cluster formation, while also noting that the sensitivity of the IMF slope to thermal feedback has a controlling influence on the outcome.

This work complements numerical studies of the IMF that explore the importance of thermal feedback, such as those of Chon et al. (2021), Guszejnov et al. (2022), Tanvir et al. (2022), and Tanvir & Krumholz (2024), as well as studies that address the dynamical influence of radiation pressure, such as Kim et al. (2018), Crocker et al. (2018b), Crocker et al. (2018a), and Menon et al. (2024). An analytical approach is useful, because of the very high dynamic range required to simulate regions as massive as globular clusters with the mass resolution required to capture fragmentation.

ACKNOWLEDGEMENTS

Very helpful comments from Chris McKee, Liang Dai, Scott Tremaine, Massimo Pascale, James Gurian, Kaitlin Kratter, Sally Oey, Mike Grudić, and the referee are all deeply appreciated. This research has been supported in part by an NSERC Discovery Grant.

REFERENCES

- Bate, M. R. 2009, MNRAS, 392, 1363
- Baumgardt, H., De Marchi, G., & Kroupa, P. 2008, ApJ, 685, 247
- Baumgardt, H., Hénault-Brunet, V., Dickson, N., & Sollima, A. 2023, MNRAS, 521, 3991
- Bertoldi, F. & McKee, C. F. 1992, ApJ, 395, 140
- Bonnell, I. A., Vine, S. G., & Bate, M. R. 2004, MNRAS, 349, 735
- Bonnor, W. B. 1956, MNRAS, 116, 351
- Breen, P. G. & Heggie, D. C. 2013, MNRAS, 432, 2779
- Burkert, A. & Bodenheimer, P. 2000, ApJ, 543, 822
- Cameron, A. J., Katz, H., Witten, C., Saxena, A., Laporte, N., & Bunker, A. J. 2023, arXiv e-prints, arXiv:2311.02051
- Chabrier, G. 2003, PASP, 115, 763
- Chabrier, G. 2005, in Astrophysics and Space Science Library, Vol. 327, The Initial Mass Function 50 Years Later, ed. E. Corbelli, F. Palla, & H. Zinnecker, 41
- Chabrier, G. & Dumond, P. 2024, ApJ, 966, 48
- Chakrabarti, S. & McKee, C. F. 2005, ApJ, 631, 792
- Chandrasekhar, S. 1931, ApJ, 74, 81
- Chon, S., Omukai, K., & Schneider, R. 2021, MNRAS, 508, 4175
- Commerçon, B., Hennebelle, P., & Henning, T. 2011, ApJL, 742, L9
- Crocker, R. M., Krumholz, M. R., Thompson, T. A., Baumgardt, H., & Mackey, D. 2018a, MNRAS, 481, 4895
- Crocker, R. M., Krumholz, M. R., Thompson, T. A., & Clutterbuck, J. 2018b, MNRAS, 478, 81
- Dib, S. 2023, ApJ, 959, 88

- Ebert, R. 1955, *ZA*, 37, 217
- Eddington, A. S. 1920, *The Observatory*, 43, 341
- El-Badry, K. & Rix, H.-W. 2019, *MNRAS*, 482, L139
- Elmegreen, B. G., Klessen, R. S., & Wilson, C. D. 2008, *ApJ*, 681, 365
- Fall, S. M., Krumholz, M. R., & Matzner, C. D. 2010, *ApJL*, 710, L142
- Fiege, J. D. & Pudritz, R. E. 2000, *MNRAS*, 311, 105
- Fujimoto, S., Wang, B., Weaver, J., Kokorev, V., Atek, H., Bezanson, R., Labbe, I., Brammer, G., Greene, J. E., Chemerynska, I., Dayal, P., de Graaff, A., Furtak, L. J., Oesch, P. A., Setton, D. J., Price, S. H., Miller, T. B., Williams, C. C., Whitaker, K. E., Zitrin, A., Cutler, S. E., Leja, J., Pan, R., Coe, D., van Dokkum, P., Feldmann, R., Fudamoto, Y., Goulding, A. D., Khullar, G., Marchesini, D., Maseda, M., Nanayakkara, T., Nelson, E. J., Smit, R., Stefanon, M., & Weibel, A. 2023, arXiv e-prints, arXiv:2308.11609
- Gammie, C. F. 2001, *ApJ*, 553, 174
- Goldsmith, P. F. 2001, *ApJ*, 557, 736
- Gratton, R. G., Carretta, E., & Bragaglia, A. 2012, *A&A Rv*, 20, 50
- Guszejnov, D., Grudić, M. Y., Offner, S. S. R., Faucher-Giguère, C.-A., Hopkins, P. F., & Rosen, A. L. 2022, *MNRAS*, 515, 4929
- Guszejnov, D. & Hopkins, P. F. 2015, *MNRAS*, 450, 4137
- Harris, W. E. 1996, *AJ*, 112, 1487
- Hennelbelle, P. & Chabrier, G. 2013, *ApJ*, 770, 150
- Hennelbelle, P., Commerçon, B., Lee, Y.-N., & Chabrier, G. 2020, *ApJ*, 904, 194
- Hopkins, P. F. 2012a, *MNRAS*, 423, 2016
- . 2012b, *MNRAS*, 423, 2037
- Hopkins, P. F., Murray, N., Quataert, E., & Thompson, T. A. 2010, *Monthly Notices of the Royal Astronomical Society: Letters*, 401, L19
- Hosek, Matthew W., J., Lu, J. R., Anderson, J., Najarro, F., Ghez, A. M., Morris, M. R., Clarkson, W. I., & Albers, S. M. 2019, *ApJ*, 870, 44
- Kenyon, S. J., Hartmann, L. W., Strom, K. M., & Strom, S. E. 1990, *AJ*, 99, 869
- Kim, J.-G., Kim, W.-T., & Ostriker, E. C. 2018, *The Astrophysical Journal*, 859, 68
- Klassen, M., Pudritz, R. E., & Kirk, H. 2017, *MNRAS*, 465, 2254
- Kratter, K. M. & Matzner, C. D. 2006, *MNRAS*, 373, 1563
- Kratter, K. M., Matzner, C. D., Krumholz, M. R., & Klein, R. I. 2010, *ApJ*, 708, 1585
- Kroupa, P. 2001, *MNRAS*, 322, 231
- Krumholz, M. R. 2011, *ApJ*, 743, 110
- Krumholz, M. R., Klein, R. I., & McKee, C. F. 2011, *ApJ*, 740, 74
- Krumholz, M. R. & McKee, C. F. 2008, *Nature*, 451, 1082
- Krumholz, M. R., McKee, C. F., & Klein, R. I. 2004, *The Astrophysical Journal*, 618, L33
- Lee, Y.-N. & Hennelbelle, P. 2018, *A&A*, 611, A89
- Lochhaas, C. & Thompson, T. A. 2017, *MNRAS*, 470, 977
- Low, C. & Lynden-Bell, D. 1976, *MNRAS*, 176, 367
- Lu, J. R., Do, T., Ghez, A. M., Morris, M. R., Yelda, S., & Matthews, K. 2013, *ApJ*, 764, 155
- Marks, M. & Kroupa, P. 2010, *MNRAS*, 406, 2000
- Marques-Chaves, R., Schaerer, D., Kuruvanthodi, A., Korber, D., Prantzos, N., Charbonnel, C., Weibel, A., Izotov, Y. I., Messa, M., Brammer, G., Dessauges-Zavadsky, M., & Oesch, P. 2024, *A&A*, 681, A30
- Masunaga, H. & Inutsuka, S.-i. 1999, *ApJ*, 510, 822
- Matzner, C. D. & Jumper, P. H. 2015, *ApJ*, 815, 68
- Matzner, C. D. & Levin, Y. 2005, *ApJ*, 628, 817
- Matzner, C. D. & McKee, C. F. 2000, *ApJ*, 545, 364
- McKee, C. F. & Zweibel, E. G. 1995, *ApJ*, 440, 686
- Menon, S. H., Lancaster, L., Burkhardt, B., Somerville, R. S., Dekel, A., & Krumholz, M. R. 2024, *ApJL*, 967, L28
- Moe, M., Kratter, K. M., & Badenes, C. 2019, *ApJ*, 875, 61
- Myers, A. T., McKee, C. F., Cunningham, A. J., Klein, R. I., & Krumholz, M. R. 2013, *ApJ*, 766, 97
- Navarro-Carrera, R., Caputi, K. I., Iani, E., Rinaldi, P., Kokorev, V., & Kerutt, J. 2024, arXiv e-prints, arXiv:2407.14201
- Nayakshin, S. & Sunyaev, R. 2005, *MNRAS*, 364, L23
- Oey, M. S. 2011, *ApJL*, 739, L46
- Offner, S. S. R., Klein, R. I., McKee, C. F., & Krumholz, M. R. 2009, *ApJ*, 703, 131
- Offner, S. S. R., Kratter, K. M., Matzner, C. D., Krumholz, M. R., & Klein, R. I. 2010, *ApJ*, 725, 1485
- Offner, S. S. R. & McKee, C. F. 2011, *ApJ*, 736, 53
- Offner, S. S. R., Moe, M., Kratter, K. M., Sadavoy, S. I., Jensen, E. L. N., & Tobin, J. J. 2023, in *Astronomical Society of the Pacific Conference Series*, Vol. 534, *Protostars and Planets VII*, ed. S. Inutsuka, Y. Aikawa, T. Muto, K. Tomida, & M. Tamura, 275
- Omukai, K. 2000, *ApJ*, 534, 809
- Ostriker, J. 1964, *ApJ*, 140, 1056
- Palla, F. & Stahler, S. W. 1990, *ApJL*, 360, L47
- Pascale, M. & Dai, L. 2024, arXiv e-prints, arXiv:2404.10755
- Pascale, M., Dai, L., McKee, C. F., & Tsang, B. T. H. 2023, *ApJ*, 957, 77
- Rees, M. J. 1976, *MNRAS*, 176, 483

- Robitaille, T. P. 2017, *A&A*, 600, A11
- Schaerer, D., Marques-Chaves, R., Xiao, M., & Korber, D. 2024, arXiv e-prints, arXiv:2406.08408
- Semenov, D., Henning, T., Helling, C., Ilgner, M., & Sedlmayr, E. 2003, *A&A*, 410, 611
- Smith, L. J., Oey, M. S., Hernandez, S., Ryon, J., Leitherer, C., Charlot, S., Bruzual, G., Calzetti, D., Chu, Y.-H., Hayes, M. J., James, B. L., Jaskot, A. E., & Östlin, G. 2023, *ApJ*, 958, 194
- Stamatellos, D. & Whitworth, A. P. 2009, *MNRAS*, 400, 1563
- Strader, J., Caldwell, N., & Seth, A. C. 2011, *AJ*, 142, 8
- Tanvir, T. S. & Krumholz, M. R. 2024, *MNRAS*, 527, 7306
- Tanvir, T. S., Krumholz, M. R., & Federrath, C. 2022, *MNRAS*, 516, 5712
- Toomre, A. 1964, *ApJ*, 139, 1217
- Topping, M. W., Stark, D. P., Senchyna, P., Chen, Z., Zitrin, A., Endsley, R., Charlot, S., Furtak, L. J., Maseda, M. V., Plat, A., Smit, R., Mainali, R., Chevallard, J., Molyneux, S., & Rigby, J. R. 2024, arXiv e-prints, arXiv:2407.19009
- Tout, C. A., Pols, O. R., Eggleton, P. P., & Han, Z. 1996, *MNRAS*, 281, 257
- Upadhyaya, A., Marques-Chaves, R., Schaerer, D., Martins, F., Pérez-Fournon, I., Palacios, A., & Stanway, E. R. 2024, *A&A*, 686, A185
- Urban, A., Martel, H., & Evans, Neal J., I. 2010, *ApJ*, 710, 1343
- Vázquez-Semadeni, E., Ballesteros-Paredes, J., & Klessen, R. S. 2003, *ApJL*, 585, L131
- Vink, J. S. 2023, *A&A*, 679, L9
- Wünsch, R., Palouš, J., Tenorio-Tagle, G., & Ehlerová, S. 2017, *ApJ*, 835, 60
- Zonoozi, A. H., Haghi, H., & Kroupa, P. 2016, *ApJ*, 826, 89